Volume 15, Number 4, 2022. pp. 417-427

Jordan Journal of Physics

ARTICLE

Development of a Radiometer for Ground-based Ultra Violet (UV)/ Cosmic Particle Characterization

Lanre O. Daniyan[a], **Matthew O. Afolabi**[a], **Ilesanmi A. Daniyan**[b] and **Felix Ale**[c]

[a] *Department of Physics and Electronics, Adekunle Ajasin University, Akungba Akoko, Ondo State, Nigeria.*

[b] *Department of Industrial Engineering, Tshwane University of Technology, Pretoria 0001, South Africa.*

[c] *National Space Research and Development Agency (NASRDA), Abuja, Nigeria.*

Doi: **https://doi.org/10.47011/15.4.11**

Received on: 04/05/2021; *Accepted on: 22/08/2021*

Abstract: The need for high-precision radiometers for the measurement of solar ultraviolet (UV) radiation triggered this research interest. This is due to the quest for the determination of the trends of terrestrial UV trends associated with the depletion of the ozone layer. This work features the development of a radiometer for the characterization of UV and ionizing radiations from the sun reaching the earth surface at a specific location. The radiations were quantified with the aid of a UV radiation sensor, Geiger tubes, a microcontroller and associated devices. Time series and location coordinates were stamped on the data records with the aid of NEO6M Global Positioning System (GPS) modules. The ionizing radiations were characterized in counts per minute (cpm), while the UV index indications were realized from the voltage output (mV) of the UV sensor using a model based on the UV index chart. The results obtained indicate that the UV index ranges from a minimum value of 0 to a maximum value of 3, while the radiation count ranges from a minimum value of 0 to a maximum value of 48 cpm for 3 days. Hence, the status of the ozone layer can be ascertained from a review of a much longer period of data gathering.

Keywords: CPM, CSV, FFF, Geiger, GPS, Ionizing, UV.

1. Introduction

The increasing trends of human activities have led to the production of gases, such as chlorofluorocarbons CFCs (CFCs) which are destructive to the ozone layer. The ozone layer in the stratosphere absorbs most of the UV radiation emitted from the sun [1]. Hence, the ozone protects the earth's surface from the intense UV radiation from the sun, which is harmful to humans and the environment. However, the generation of gases, which depletes the ozone layer, upsets the natural balance of ozone, thus resulting in a decline in the ozone levels in the stratosphere. These reduced ozone levels have increased the amount of harmful ultraviolet radiation reaching the earth's surface [1]. Since the sun is the major propelling force of the terrestrial atmospheric processes, the variations in the atmospheric processes can be traced to the variations which arise as a result of solar radiation and its modulation by the earth's orbital motion [2-3]. Some of these variations are caused by the cosmic rays, which stem from the galactic and solar sources. The constituents of cosmic rays include high-speed neutrons, electrons and atomic nuclei. Cosmic-ray particles are mostly

Corresponding Author: Lanre O. Daniyan **Email**: danomartins@hotmail.com

comprised of fully ionized elements, such as hydrogen (87-90%) and some helium (9-12%) with small amounts of electrons (1%) [4-5]. Cosmic-ray energy level ranges between 300 MeV and 10 GeV [4]. The primary cause of modulation of cosmic rays has been traced to the variation in the magnitude of the solar wind. Hence, the variations in the UV radiation call for the need for high-precision radiometers for the measurement of solar ultraviolet (UV) radiation in order to determine the terrestrial UV trends associated with the depletion of the ozone layer. The isotopic composition of the cosmic rays provides important information about the source, acceleration and transport phenomenon of cosmic rays in the galaxy.

The knowledge of the elemental composition of cosmic rays will assist in the determination of the chemical fractionation in the source region. This will also provide information about the nature of the source region as well as the propagation of cosmic rays in the interstellar space [5]. The identification of the cosmic-ray isotopes will further enhance the understanding of the nature of the source region as well as the timescales of the injection and initial acceleration. Measurements at high energies will indicate the sources of the particles. At the highest energies, the presence of cosmic rays may indicate the approximate direction of the most powerful source [5]. Cosmic rays and energetically charged particles in space influence some occurrences in the solar atmosphere, heliosphere and geosphere. The characterization of the particles is necessary in order to understand the changes in the physical state of the magnetosphere, study the effects of space radiations on humans and the environment and understand the electromagnetic propagation in the environment [6-8].

At the core of the sun, energy is generated *via* thermonuclear reactions, creating extreme temperatures deep within the sun's core [3]. This results in a continuous emission of solar particles, ionizing radiations, Corona mass ejections, solar winds, solar flares, plasmas and other high-energy cosmic particles spanning the full electromagnetic spectrum that travel through the heliosphere. Some of these particles are absorbed, re-emitted at lower energies or intercepted within the interplanetary space.

The stratospheric ozone blocks some of these dangerous particles from reaching the earth's surface in quantities considered very dangerous to life on earth [9]. Thus, the dynamic nature of the ozone layer underscores the need to constantly monitor the quantity of radiations reaching the earth surface. Furthermore, the issue of climate change with increasing global warming has been traced to the net imbalance in the energy radiation of the earth [10]. In addition, a striking increase in the cases of skin cancers has been detected in fairly skinned populations worldwide since the early 1970s and the rising cases have been heavily linked to sun exposure and its ultraviolet (UV) component [10]. Other exposure risks include acute and chronic skin disorder such as sunburn, tanning, eye disorder, such as cataracts and photokeratitis as well as immune system disorders … etc.

Small quantities of UV radiation are needed for the production of vitamin D, which is beneficial to the human health. It is also needed in small amounts in the treatment of some disorders and diseases, such as rickets, psoriasis and eczema under proper medical supervision. However, there are some major health risks associated with the prolonged exposure to UV. Continuous exposure to UV in the long term could also induce degenerative changes in cells, fibrous tissue and blood vessels, which could lead to premature skin ageing. UV radiation can also cause inflammatory reactions of the eye, such as photokeratitis [10-11]. The aim of this study is to develop a radiometer for ground-based UV / cosmic particle characterization by integrating a UV sensor, a Geiger counter, a Global Positioning System (GPS) module and a Secure Digital (SD) memory card to a central microcontroller. The development of a high-precision ground-based radiometer will provide the relevant information about the trends of the UV levels over a period. The information about the UV levels acquired by the radiometer can also be employed for the evaluation of radiative transfer models.

The succeeding sections present a literature review in order to explore the research gaps, the materials and methods employed in this study as well as the results obtained, the conclusions and directions for future study.

2. Literature Review

Many works have been reported in an effort to estimate the magnitude of cosmic ray and characterize its particles. For instance, Simonsen *et al.* [12] developed a ground-based Galactic Cosmic Ray (GCR) simulator aimed at generating a spectrum of ion beams that approximates both the primary and secondary GCR fields experienced at human organ locations in order to mitigate the health risks due to exposure to cosmic rays. Slaba *et al.* [13] developed a preliminary beam-selection strategy for accelerator-based GCR simulation. Utomo [4] found a strong - but inverse - correlation relationship between the solar activity and cosmic rays as well as a strong and positive correlation between the solar activity and solar constant. As reported by Utomo [4], an increase in the magnitude of cosmic rays produces a decline in the solar constant. When cosmic-ray particles with high energy (10 GeV) enter the earth's atmosphere at a speed near to $3 \times 10^8\ m/s$, there is a possibility of collision with the atmospheric molecules. The collision may cause the composition of the molecules in the atmosphere to break, thereby forming secondary ions which act as condensation nuclei. Hence, this phenomenon can bring about an increase in the rate of cloud formation with subsequent reduction in the intensity of solar radiation that reaches the earth's surface. Marinan *et al.* [14] assessed a radiometer calibration with GPS radio occultation for the MiRaTA CubeSat mission. An initial estimation of the retrieved temperature precision indicated that the developed system should meet the requirements for the Global Positioning System Radio Occultation (GPSRO) temperature precision based on the thermal noise contribution of error. Mendonça *et al.* [15] analyzed the atmospheric effects of cosmic rays and the underlying relationships to cut-off rigidity and zenith angle. The analysis was carried out using Global Muon Detector Network, which consists of four multidirectional muon detectors placed at different locations, between 2007 and 2016. The results obtained indicated that the main atmospheric effects are related to pressure and temperature changes. Part *et al.* [16] developed a UV index sensor - based device with the EUVB ratio of natural light. The developed device demonstrated the capacity to acquire UV-related information, such as UVI and EUVB, which are critical to the prevention of potential damage due to exposure to UV radiation.

In this work, a UV/ cosmic particle meter was developed to characterize in real time UV and cosmic ionizing radiations reaching the earth's surface at a specific location. Alongside the times of events and the specific location coordinates, the quantities of these radiations were logged in an SD card. There is a dearth of information relating to the development of a UV/ Cosmic particle meter, which has the capacity to characterize in real time UV and cosmic ionizing radiations reaching the earth's surface at a specific location alongside the times of events and the specific location coordinates. The concept of additive manufacturing was explored in the development of the casing, which makes its process of development time- and cost-effective and easy for rapid prototyping. The development and use of the UV/ cosmic particle meter will definitely provide insight into the state, permeability and dynamics of the ozone layer. It will also strengthen sun-protection programmes and increase the awareness of the health hazards of UV radiation. This will assist people to change their lifestyle and habits in order to reduce the chances of the health risk associated with undue exposure to UV. Following a reliable means of UV measurement, effective sensitization programs can be developed in order to enhance the public health and the general approach to sun protection.

3. Materials and Methods

The developed radiometer employs the principles of spectroadiometric measurement for the characterization of the UV and ionizing radiations from the sun reaching the earth surface at a specific location. The choice of the spectroadiometric measurement stems from the problem to be addressed; ground-based Ultra Violet (UV)/ cosmic particle characterization. The ground-based measurement developed in this study is essential for proper understanding of the factors which affect the transmission of UV radiation *via* the atmosphere. It is also necessary for the evaluation of the effects of UV radiation on both the earth's ecosystems and human health [1]. The developed ground-based radiometer which employs the principles of spectroadiometric measurement is useful for detecting the UV trends and is also capable of data acquisition for the development and evaluation of radiative transfer models.

Comparing the spectral and broadband measurements, spectral measurement employed in this study boasts the effective computation of biological impacts of UV radiation for any action spectrum and of the acquisition the information on the atmospheric composition given by the fine structure of the spectrum. It is also flexible in application and eliminates spectral mismatch. However, it requires the expertise of the operator in order for effective calibration and measurement before reliable results can be obtained. On the other hand, the broadband measurement is limited only to one action spectrum, being designed to strictly follow and rely on theoretical correction factors to compensate for the spectral difference between the meter response and the desired action spectrum in order to obtain the estimates for various effects following different action spectra. However, the merits of the broadband measurement include simplicity of operation and cost effectiveness.

The materials employed for the development of the radiometer are presented in Table 1.

TABLE 1. Materials employed for the development of the radiometer.

S/N.	Material	Quantity
1.	UV sensor (ML8511)	1
2.	SD card	1
3.	Geiger counter (D-v1.1(CAJOE) with tube series J3058 2020I)	1
4.	Microcontroller (Atmel ATMega328P)	1
5.	GPS module	1
6.	Step up (LM6009)	1
7.	Li-ion 18650 batteries	4
8.	Polyethylene Terephthalate Glycol (PETG) filament for casing (building volume: 200x200x180 mm)	½ roll

3.1 System Architecture

The system architecture of the developed UV/ cosmic particle meter for the characterization of the cosmic ionizing radiation is presented in Fig. 1. The UV sensor detects the UV radiation variabilities and sends corresponding signals to the microcontroller for processing. The Geiger tube detects ionizing radiations from the sun and sends the corresponding pulse counts to the microcontroller, which in turn counts the frequencies in number of occurrences per minute (cpm). Subsequently, the UV index is computed from the UV voltage levels by the microcontroller through a pre-programmed UV index chart. The date, as well as the time series are extracted from the GPS NMEA sentences and logged with the UV and Geiger data onto the SD card in CSV format.

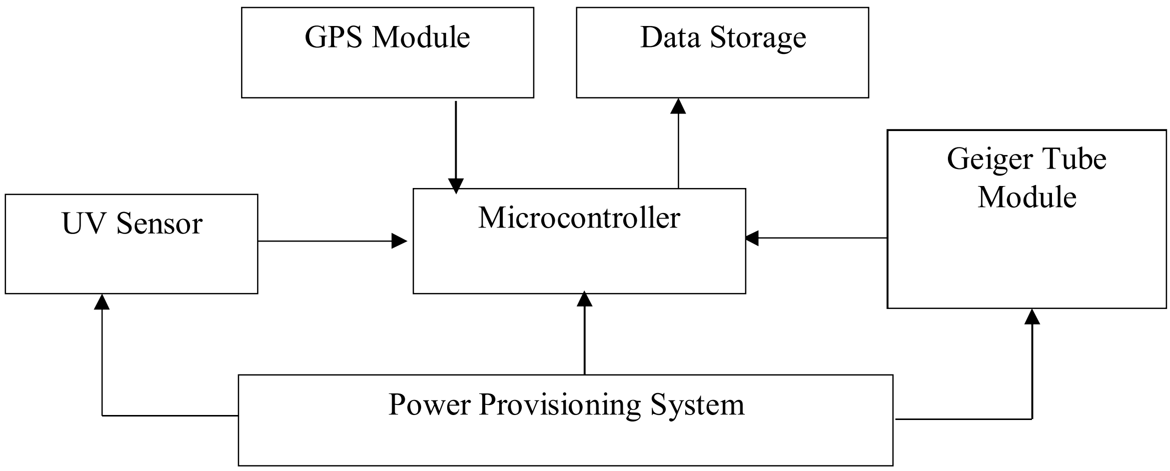

FIG. 1. Architecture of the UV/ cosmic particle meter.

3.2 Proteus Model

Fig. 2 presents the Proteus model of the system circuitry, which depicts the connection of the Geiger counter, GPS, memory and UV sensors to the central microcontroller.

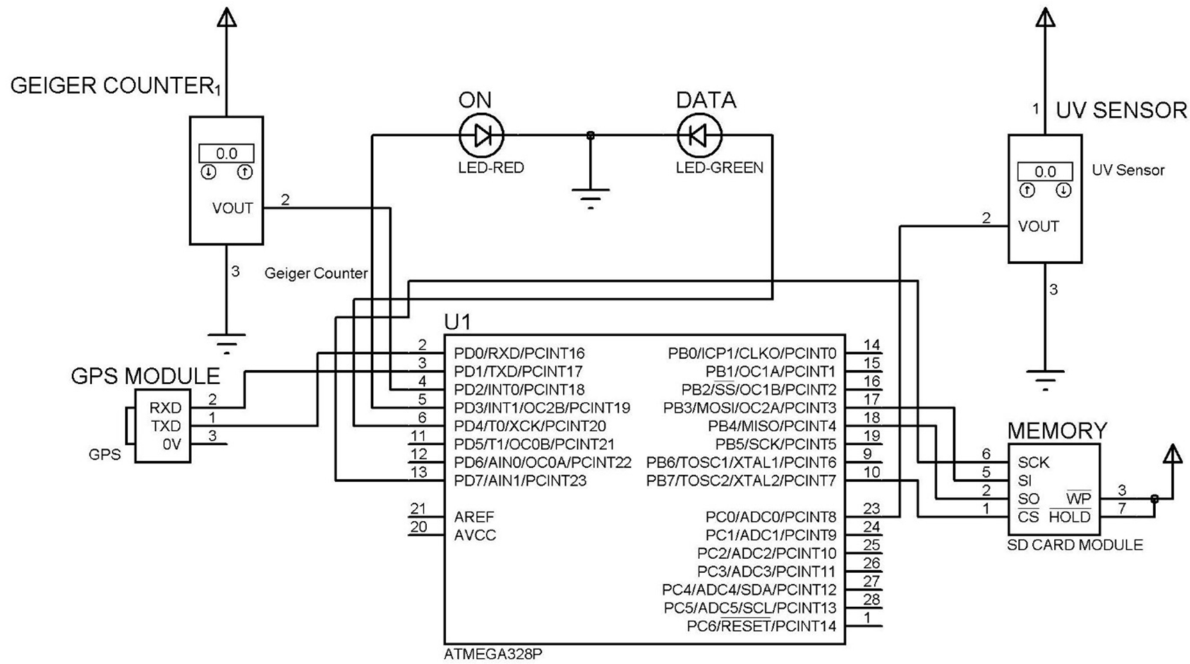

FIG. 2. Proteus model of the system circuitry.

3.3 Material Consideration

For the implementation of this design, the following materials were considered.

1. A UV sensor ML8511 was used. This sensor outputs analog voltage that is linearly related to the measured UV intensity (mW/cm^2) in the range of 200 – 375 nm wavelength. This module with an input voltage range of 3.3 – 5 V has an output voltage range of 0 – 1 V. The ML8511 is equipped with an amplifier, which converts photocurrent into voltage depending on UV intensity[17]. Its normal environmental working temperature range is -20 to 85°C.
2. A Geiger radiation counter D-v1.1(CAJOE) with the tube series J3058 2020I was employed for picking the doses of ionizing radiation. A Geiger counter is a device used for detecting and measuring ionizing radiation. The tube is filled with an inert gas that becomes conductive when it is impacted by a high – energy particle [18]. The tube with a diameter of 10 mm and a length of 90 mm has a starting voltage of about 350 V, an operational voltage of about 380 V and an extreme voltage of about 550 V. It is very suitable for environments with temperatures of about -40 - 55°C. The tube has a chamber containing two electrodes and a potential difference of several hundred volts and is also filled with inert gas at low pressure. A charged particle passing through the gas causes excited and ionized molecules along its path [19]. With the high voltage and consequently the strong electric field, there is a resultant conduction in the tube.
3. LM6009 boost converter steps up the voltage from about 3.7 V provided by an array of Li-ion to a regulated 5 V needed to operate the system. This converter has an input range of 3–32 V, an output range of 5–35 V and a maximum output current of 4 A [20].
4. An Atmel ATMega328P microcontroller was programmed to count the pulse input from the Geiger counter module and receive input from the UV sensor and the time-location strings from the NEO6M GPS module. ATMega 328P is an 8 – bit AVR microcontroller with 32Kbytes in-system programmable flash [21].
5. Other materials include Li-ion 18650 batteries and an SD card module for data storage.

The ATmega 328p microcontroller was employed as the central controller. This microcontroller was installed on a circuit board developed using a vero board. The microcontroller is comprised of 14 digital pins and 6 programmable analog inputs. The outputs of the UV sensor are fed into the microcontroller alongside the time-location strings from the GPS. The microcontroller is programmed to count the pulse input from the Geiger counter module.

3.4 Casing Fabrication

The casing was modelled using Rhinoceros, a Computer-aided Design (CAD) environment for 3D modeling. The 3D model was subsequently sliced using CURA slicer with a 0.1-mm layer height configuration. The resultant G-code was fed into Whanhao duplicator i3 plus, for fused filament fabrication *via* the process of additive manufacturing. Whanhao duplicator i3 plus is a single-extruder system with a building volume capacity of 200x200x180 mm [22]. Fig. 3 presents the block diagram for the additive manufacturing process. The additive manufacturing (AM) is an emerging digital technology capable of producing component parts directly from a digital model [23-24]. The 3D model was implemented using sky blue and white PETG filament *via* additive manufacturing to realize the casing.

The model shown in Fig. 4 was implemented using the additive manufacturing technique. The final product is shown in Fig. 4.

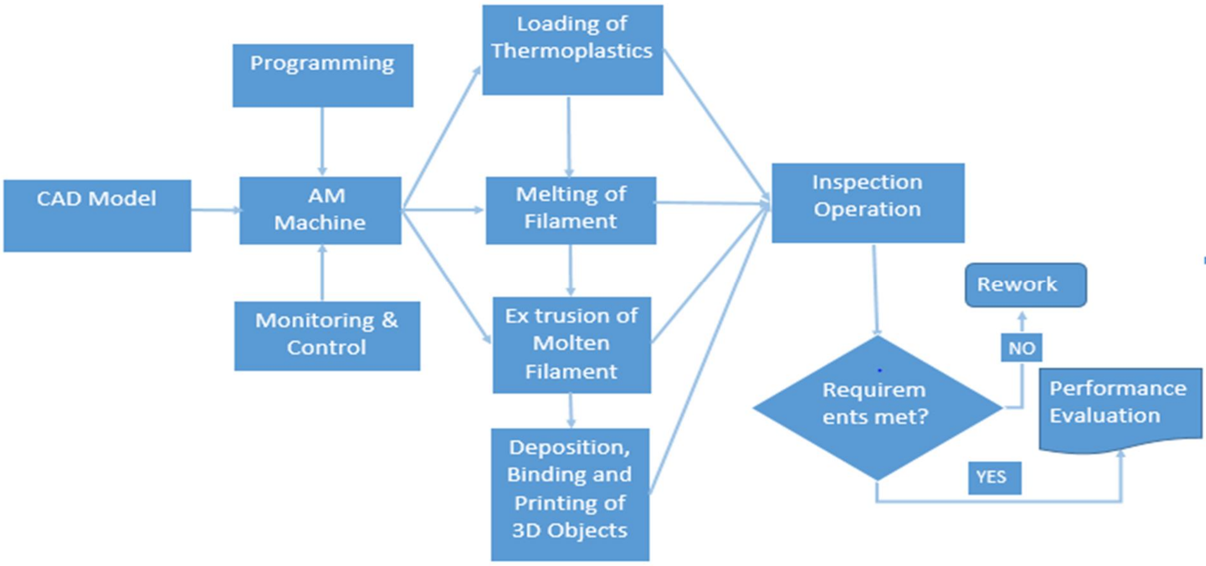

FIG. 3. Block diagram for the additive manufacturing process [25].

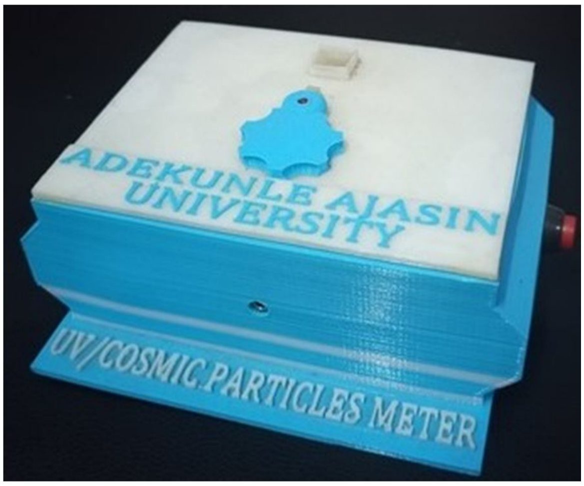

FIG. 4. The UV/ cosmic particle meter.

3.5 Performance Evaluation of the Radiometer

The radiometer characterizes UV and ionizing radiation from the sun reaching the earth surface at a specific location. The intensity of these cosmic radiations depends on the time of the year, the geographical location and the dynamics of the ozone layer the state of which determines its permeability to radiations. These radiations were quantified with the aid of a UV radiation sensor, Geiger tubes, a Microcontroller and associated devices. Data is stored in an SD card in Comma Separated Version (CSV) format for future processing. Time-series and location coordinates were stamped on the data records with the aid of NEO6M GPS modules. The ionizing radiations were characterized in counts per minute (cpm), while the UV index indications were realized from the voltage output (mV) of the UV sensor using a model based on the UV index chart. The characterization of UV and ionizing radiations were carried out at a specific location between 10 am and 2 pm and at an update cycle of five minutes for a test period of three days. The geographical features of the location are as follows: latitude: 6.84, longitude: 7.35, altitude: 432 m, as indicated by the GPS subsystem.

Eq. (1) expresses the global solar UV index (CIE: ISO 17166:1999/CIE S 007/E-1998) which measures the UV radiation.

$$I_{UV} = k_{er}.\int_{250\ nm}^{400\ nm} E_\lambda.S_{er}(\lambda)d\lambda \quad (1)$$

where E_λ is the solar spectral irradiance ($W/(m^2.nm^1)$, (λ) is the wavelength and $d\lambda$ is the wavelength interval. S_{er} is the erythema reference action spectrum and k_{er} is a constant equal to 40 m^2/W.

The mean rate of change of momentum of an individual particle, as given by the adiabatic deceleration rate, is expressed by Eq. (2) [26]:

$$\dot{P}_{ad} = \frac{-p^i}{3}\frac{\partial}{\partial r}.V \quad (2)$$

where p^i is the particle momentum (kg m/s) and V is the solar-wind velocity (m/s) at a position r.

Eq. (3) expresses the mean rate of change of momentum of the cosmic-ray particles having momentum p^i specified relative to the wind frame at position r [26].

$$(\dot{p^i})^* = \frac{-P^i}{3}\frac{\partial}{\partial r}.V \quad (3)$$

Considering the particle streaming and energy changes, the continuity equation for the cosmic rays which propagate in the interplanetary region is expressed by Eq. (4).

$$\frac{\partial (U_p)^*}{\partial t} + \frac{\partial}{\partial r}.(S_P)^* + \frac{\partial}{\partial p^i}\left((\dot{p}^i)^*(U_p)^*\right) = 0 \quad (4)$$

where r is the position, p^i is the particle momentum (kg m/s), $(U_p)^*$ is the differential number density and $(S_P)^*$ is the differential current density.

Eq. (5) expresses the time rate of change of momentum of the particles in the fixed frame [5].

$$\dot{p} = \frac{p}{3U_p}V.\frac{\partial U_p}{\partial r}. \quad (5)$$

For spectroradiometric measurement, Eq. (6) holds [1]:

$$S(A, \Delta\lambda, \lambda_o) = \int_{\Delta\lambda}^{\infty}\int_{A}^{\infty} E_\lambda(x, y, \lambda)R_\Phi(\lambda_o, \lambda)dAd\lambda \quad (6)$$

where E_λ is the spectral irradiance (w/m^3) measured at points $x\ and\ y$ and at a wavelength λ (nm). R_Φ is the flux responsivity of the spectroradiometer (V/W), $\Delta\lambda$ is the bandwidth of the spectroradiometer (bps) and A is the area of the receiving aperture (mm^2).

For a homogeneous field, Equation 6 reduces to Eq. (7) [1].

$$S(\lambda_o) = A\int_{\Delta\lambda}^{\infty} E_\lambda(\lambda)R_\Phi(\lambda_o, \lambda)d\lambda. \quad (7)$$

The bandwidth of the measurement instrument is determined using Eq. (8) [1].

$$\Delta\lambda = \frac{\int_{\Delta\lambda}^{\infty} R_\Phi(\lambda_o,\lambda)d\lambda}{R_\Phi(\lambda_o,\lambda)}. \quad (8)$$

The radiometer uses a Geiger tube J305 202I which is largely used for the detection of beta and gamma radiations. The Geiger tube contains a low-pressure inert gas, usually helium, neon or argon, thus making the Geiger tube non-conductive under normal conditions. Whenever the tube receives cosmic-ionizing radiation reaching the earth's surface, the gas is ionized; electrons are stripped off the inert gas molecules, thus making the inert gas conducting across the electrodes which have a potential difference of about 500 Volts across the terminals. When the gas molecules are ionized, positively charged ions and electrons are created. A strong electric field is created by the tube's electrodes, accelerating the ions towards the cathode and the electrons towards the anode. The ion pairs gain sufficient energy to ionize further gas molecules through collisions on their way, thereby creating an avalanche of charged particles. This momentary occurrence generates a pulse of current which passes from the negative electrode to the positive electrode and is counted per time by the microcontroller. The counts per minute (cpm) alongside the ultraviolet radiation mV reading and the corresponding UV index are logged in a csv file.

4. Results and Discussion

Fig. 5 shows the output from the UV sensor (mV), while Fig. 6 shows the corresponding UV index chart. These variations were between 10 am and 2 pm at an update cycle of 5 minutes for a period of three (3) days at a specific location: latitude: 6.84, longitude: 7.35, altitude: 432 m, as indicated by the GPS sub-system.

The noticeable correlation in the two Figs. (5 and 6) shows that the modeling of the UV index chart by the instrument based on the output of the UV sensor and the UV index chart were quite good enough to give an understanding of safety levels, appropriate response and precautionary measures to be taken at certain exposure levels. The good fit in Fig. 5 for the three days under review is also an indication of good repeatability of the characterizing instrument. The UV index ranges from a minimum value of 0 to a maximum value of 3. According to the Global Solar UV Index report, [10], values ranging from 0 to < 2 are considered low with no protection required. On the other hand, values ranging from 3-5 are considered moderate with some level of protection required. It is then implied from the results obtained that the UV radiation ranges from low to moderate with some level of protection required in cases where the magnitude of the UV index exceeds 2. Global Solar UV Index report [10] identifies the factors which influence the UV levels, such as sun elevation, latitude, cloud cover, altitude, ozone layer and ground reflection. An increase in the altitude will result in an increase in the UV index and the closer the latitude to the equatorial regions, the higher the UV-radiation levels and *vice versa*. The higher the sun in the sky, the higher the UV-radiation level and *vice versa*. The UV-radiation levels vary with the time of the day and the time of the year. The highest level of the UV-radiation is usually obtained when the sun is at its maximum elevation outside the tropics and at around the midday (solar noon) during the summer months. The presence of clouds reduces the UV levels as UV-radiation levels are highest under cloudless skies. However, even with cloud cover, the UV-radiation levels can be sometimes high. The effect of scattering can have the same effect as the reflectance by different surfaces hence increasing the total UV-radiation levels [10]. The presence of the ozone layer also reduces the level of UV radiation. The ozone layer can absorb some of the UV radiation that would otherwise reach the earth's surface. In the event of continuous depletion of the ozone layer, gradual increase in the mV reading, the UV index and the frequency of occurrence of ionizing radiation in cpm, over time, would be the indications. Also, if these parameters drop in values recorded over time, this would suggest the healing of the ozone layer.

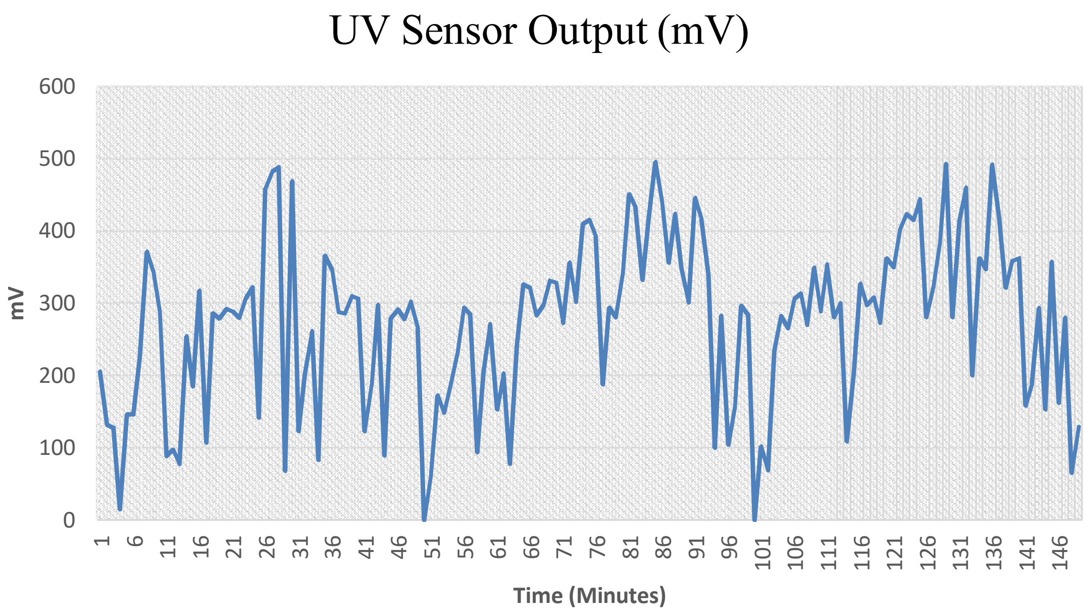

FIG. 5. Variations of the UV sensor (mV).

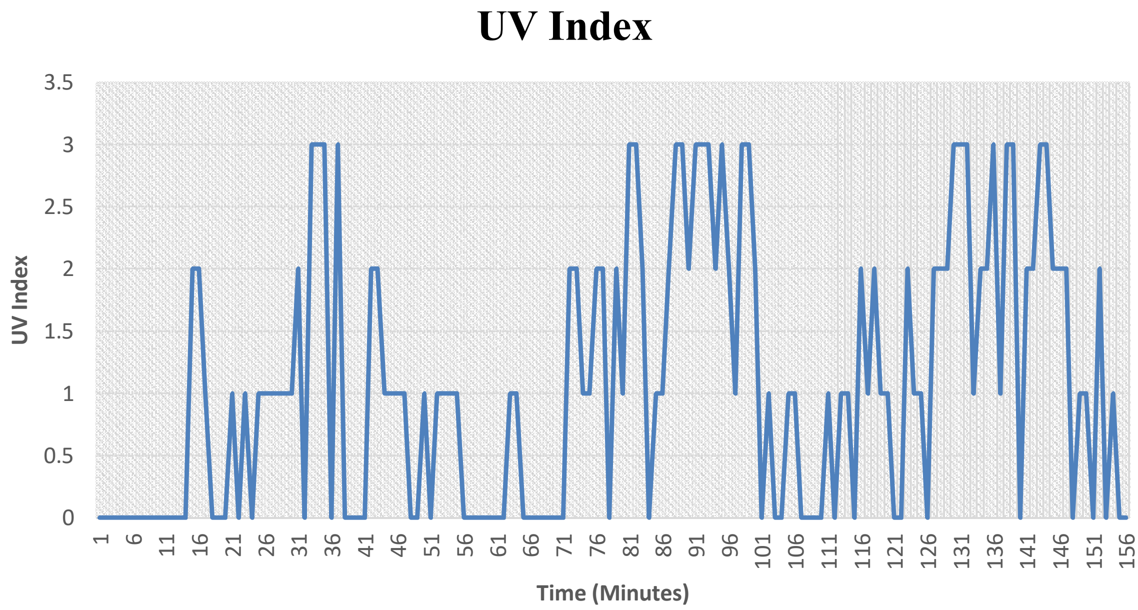

FIG. 6. UV index variations.

Fig. 7 shows the frequency of arrival of cosmic ionizing radiations in counts per minute as detected by the Geiger counter sub-system at a specific location: latitude: 6.84, longitude: 7.35, altitude: 432 m, as indicated by the GPS sub-system. These variations are between 10 am and 2 pm and at an update cycle of five minutes for a test period of three days. These variations over a much longer period of time would provide insights into the status and dynamics of the ozone layer and its permeability to UV radiations around the equatorial region through the ground-based measurement approach. The standard unit of radiation dose in an area is measured in micro-Sievert/hour (µSv/hr). Hence, the result obtained for the counts per minute (CPM) is multiplied by 0.0057 to obtain its equivalent radiation level in µSv/hr [27]. This implies that the radiation dose in the area ranges from a minimum value of 0 to a maximum value of 0.2736 µSv/hr for a period of 3 days.

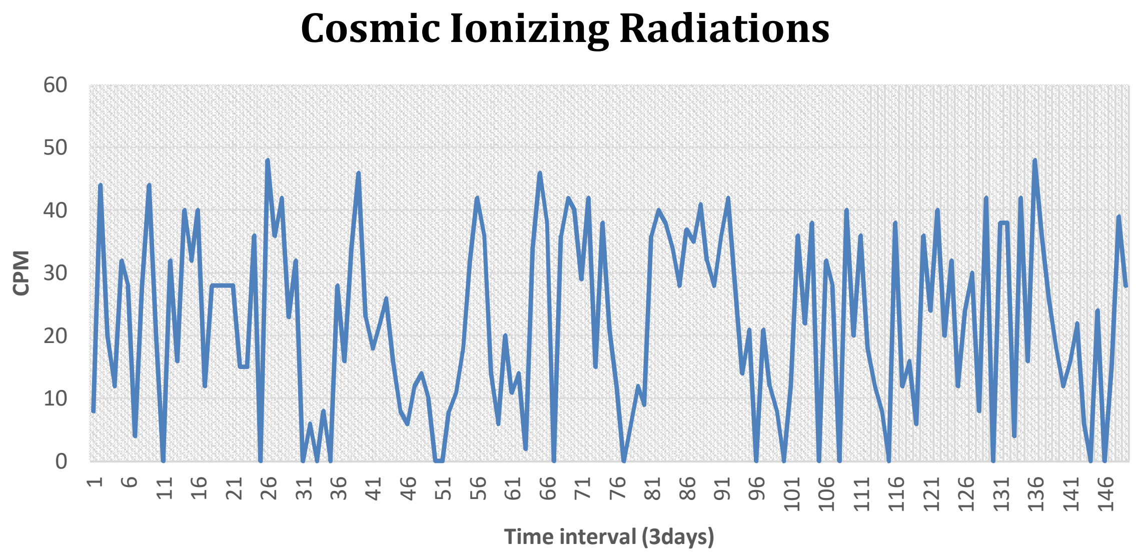

FIG. 7. Cosmic ionizing radiation variations.

The maximum mean body effective dose limit is 20 milliSieverts (mSv) per year (averaged over 5 years) [28-29]. This is recommended for people exposed to radiation as part of their occupation (including air-flight crew), while 1 mSv/year is recommended for the general population. More performance evaluation of the developed radiometer should be carried out over the period of at least one year in order to obtain the average cosmic radiation, so that comparison analysis can be carried out with the recommended standards. This will also give an indication of the permeability of the ozone layer to cosmic particles.

5. Conclusion

The aim of this study was to develop a radiometer for ground-based UV/ cosmic particle characterization. This was achieved by integrating a UV sensor, a Geiger counter, a GPS module and an SD memory card to a central microcontroller. The casing of the system was developed additively using the PETG filament. The results obtained indicate that the UV index ranges from a minimum value of 0 to a maximum value of 3, while the ionizing radiation count ranges from a minimum value of 0 to a maximum value of 48 cpm for 3 days under review. The results obtained from the performance evaluation also indicate that the UV index chart was quite good enough to give an understanding of safety levels, appropriate response and precautionary measures to be taken at certain exposure levels. The good fit for the three days review is also an indication of good repeatability of the characterizing instrument. Following a reliable means of UV measurement and Geiger counts, it is envisaged that adequate inference could be drawn from a review of much longer period of data gathering, with a view to ascertain the status of the ozone layer. The UV and cosmic ionizing radiation variations over a much longer period would provide insights into the status and dynamics of the ozone layer and its permeability to cosmic radiations around the equatorial region through the ground-based measurement approach.

Also, effective sensitization programs can be developed in order to enhance the public health and the general approach to sun protection. It is envisaged that the use of the developed system will enhance the particle characterization of cosmic rays. Future works can consider a review of at least two years.

References

[1] Leszczynski, K., "Assessment and Comparison of Methods for Solar Ultraviolet Radiation Measurements", (Helsinki, 1995), pp. 1-69.

[2] Bolonkin, A. and Friedlander, J., Scientific Research Journal of Computational Water, Energy and Environmental Engineering, 2 (2013) 83.

[3] The Universe Today “Characteristics of the Sun”, Space and Astronomy New, [Online]. www.universetoday.com/94252/characteristics-of-the-sun/. Retrieved on 6th March, 2012.

[4] Utomo, Y.S., Journal of Physics: Conf. Series, 817 (2017) 012045.

[5] International Space Science Institute, "Cosmic Rays", (Association Pro ISSI, Zurich, 2003), pp. 1-16.

[6] Kudela, K., 30th International Cosmic Rays Conference, Merida, Mexico, (2007).

[7] Putze, A., Master Thesis, Physics and Engineering: Sub-atomic Physics and Astroparticles, Joseph Fourier University at Grenoble, (2006), France.

[8] Goldhagen, P., Clem, J.M. and Wilson, J.W., Radiation Protection Dosimetry, 110 (1-4) (2004) 387.

[9] National Research Council (NRC). Health risks from exposure to low levels of ionizing radiation. BEIR VII Phase 2 report. National Academies Press; (2006). 3. Durante M. and Cucinotta, F.A., Physical basis of radiation protection.

[10] NASA, “Chemistry of the Ozone”, (2013).

[11] Global Solar UV Index: A Practical Guide, World Health Organisation, (2002), Geneva, Switzerland.

[12] Simonsen, L.C., Slaba, T.C., Guida, P. and Rusek, A., PLoS Biol., 18 (5) (2020) 1.

[13] Slaba, T.C., Blattnig, S.R., Norbury, J.W., Rusek, A. and La Tessa, C., Life Sciences in Space Research, 8, (2016) 52.

[14] Marinan, A.D., Cahoy, K.L., Bishop, R.L., Lui, S.S., Bardeen, J.R., Mulligan, T., Blackwell, W.J., Leslie, R.W., Osaretin, I.A. and Shields, M., IEEE Journal of Selected Topics In Applied Earth Observations and Remote Sensing, 9 (12) (2016) 5703.

[15] Mendonça, R.R.S., Wang, C., Braga, C.R., Echer, E., Lago, A.D., Costa, J.E.R., Munakata, K., Li, H., Liu, Z., Raulin, J-P., Kuwabara, T., Kozai, M., Kato, C., Rockenbach, M., Schuch, N-J., Al-Jasser, H.K., Sharma, M.M., Tokumaru, M., Duldig, M.L., Humble, J.E., Evenson, P. and Sabbah, I., Journal of Geophysical Research: Space Physics, 124 (2019) 9791.

[16] Park, D-H., Oh, S-H. and Lim, J-H., Sensors, 19 (754) (2016) 1.

[17] LAPIS Semiconductor, "ML8511 Datasheet", FEDL8511 – 05, March, (2013).

[18] Project Hub, "Geiger Counter with Arduino Uno", DEEDU/ Erasmus/ European Commission Project no. 2018-1 FR02 – KA205 – 014144, Jan (2018).

[19] Tysk, C., Olsson, A. and Brenner, E., "Construction of a Geiger Counter for Cosmic Radiation Measurement in near Space Conditions", (Uppsala University, June 2018).

[20] KimGrity, "LM6009 S DC-DC Power Step-up Module 3 – 34V to 4 – 35V DIY Module" [Online], www.kimgrity.com/dccdc-coverter. Retrieved on 6th March, (2012).

[21] Atmel, "ATMega328P" ATMega328P Datasheet 7810D-AVR, Jan (2015).

[22] Wanhao, "3D Printer I3 Plus Instruction Manual", Model: Duplicator I3.

[23] Daniyan, I.A., Mpofu, K., Oyesola, M.O. and Daniyan, L., Procedia CIRP, 95 (2020) 89.

[24] Daniyan, I.A., Balogun, V., Mpofu, K. and Omigbodun, F.T., International Journal on Interactive Design and Manufacturing, 14 (2020) 651.

[25] Daniyan, I.A., Mpofu, K., Daniyan, O.L., Fameso, F. and Oyesola, M., The International Journal of Advanced Manufacturing Technology, 107 (2020) 4517.

[26] Webb, G.M. and Gleeson, L.J., Journal of Astrophysics and Space Science, 60 (2) (1979) 335.

[27] Parlante, N. (2012). Nick's Geiger Counter Page. [Online], Availale at: https:// cs.stanford.edu/people/nick/geiger. Accessed on 13th August, 2021.

[28] Walker, S.A., Townsend, L.W. and Norbury, J.W., Space Res., 51 (2013) 1792.

[29] International Commission on Radiological Protection (ICRP), ICRP Publication 136, Ann. ICRP, 46 (2) (2017) 1.